

Synchronization of multi-frequency noise-induced oscillations

Sergey Astakhov, Alexey Feoktistov, Vadim S. Anishchenko, and Jürgen Kurths

Citation: *Chaos* **21**, 047513 (2011); doi: 10.1063/1.3659281

View online: <http://dx.doi.org/10.1063/1.3659281>

View Table of Contents: <http://chaos.aip.org/resource/1/CHAOEH/v21/i4>

Published by the [American Institute of Physics](#).

Related Articles

Exponential synchronization of stochastic neural networks with leakage delay and reaction-diffusion terms via periodically intermittent control

Chaos **22**, 013124 (2012)

On the variational homotopy perturbation method for nonlinear oscillators

J. Math. Phys. **53**, 024101 (2012)

Multistability of twisted states in non-locally coupled Kuramoto-type models

Chaos **22**, 013114 (2012)

Theoretical analysis of multiplicative-noise-induced complete synchronization in global coupled dynamical network

Chaos **22**, 013110 (2012)

Propagation of spiking regularity and double coherence resonance in feedforward networks

Chaos **22**, 013104 (2012)

Additional information on Chaos

Journal Homepage: <http://chaos.aip.org/>

Journal Information: http://chaos.aip.org/about/about_the_journal

Top downloads: http://chaos.aip.org/features/most_downloaded

Information for Authors: <http://chaos.aip.org/authors>

ADVERTISEMENT



Submit Now

**Explore AIP's new
open-access journal**

- **Article-level metrics
now available**
- **Join the conversation!
Rate & comment on articles**

Synchronization of multi-frequency noise-induced oscillations

Sergey Astakhov,^{1,a)} Alexey Feoktistov,¹ Vadim S. Anishchenko,¹ and Jürgen Kurths^{2,3}

¹*Saratov State University, 410012 Saratov, Russia*

²*Potsdam Institute for Climate Impact Research (PIK), 14473 Potsdam, Germany*

³*Institute for Complex Systems and Mathematical Biology, University of Aberdeen, Aberdeen AB243UE, United Kingdom*

(Received 12 August 2011; accepted 19 October 2011; published online 29 December 2011)

Using a model system of FitzHugh-Nagumo type in the excitable regime, the similarity between synchronization of self-sustained and noise-induced oscillations is studied for the case of more than one main frequency in the spectrum. It is shown that this excitable system undergoes the same frequency lockings as a self-sustained quasiperiodic oscillator. The presence of noise-induced both stable and unstable limit cycles and tori, as well as their tangential bifurcations, are discussed. As the FitzHugh-Nagumo oscillator represents one of the basic neural models, the obtained results are of high importance for neuroscience. © 2011 American Institute of Physics. [doi:10.1063/1.3659281]

One of the basic models in neuroscience is the FitzHugh-Nagumo oscillator, which describes the excitable dynamics of a single neuron. In the excitable regime, under the influence of noise the model demonstrates the phenomenon of Coherence Resonance: the oscillations become coherent at certain noise intensity. It is well known that such oscillations can be synchronized by an external harmonic force and even mutual synchronization may appear when a pair of non-identical oscillators is coupled. Using numerical simulations and electronic experiments, we show that the noise-induced oscillations with few main frequencies in excitable systems of the FitzHugh-Nagumo type demonstrate a kind of synchronization which obeys the same scenario as the synchronization of deterministic self-sustained quasiperiodic oscillations. This enables us to predict the existence of stable and unstable noise-induced limit cycles and tori which should possess similar tangential bifurcations as in the case of quasiperiodic oscillations.

I. INTRODUCTION

Synchronization is a fundamental phenomenon in non-linear sciences¹ which takes place in a wide range of fields: mechanics,² electronics,³ biology⁴ and neuroscience,^{5,6} chemistry,^{7,8} Earth sciences,^{9–11} economics,¹² sociology,¹³ etc. Synchronization can be observed in different types of dynamic regimes: periodic, quasi-periodic, chaotic, and stochastic. In this paper, we consider synchronization through frequency-locking mechanisms. We analyze the route to synchronization of noise-induced coherent oscillations in excitable systems with one and more main peaks in the Fourier spectrum and compare it with the case of periodic and quasiperiodic self-sustained oscillations in deterministic systems.

We show that in the case of noise-induced oscillations the synchronization route through frequency locking is quite

similar to the route observed in deterministic self-sustained oscillations in both periodic and quasi-periodic cases. As the saddle-node bifurcations of limit cycles and invariant tori underly the synchronization mechanism in the deterministic case, we assume that noise-induced stable and saddle limit-cycles and tori may exist in an excitable system under the influence of noise as well and undergo saddle-node bifurcations.

II. THE ROLE OF SADDLE-NODE BIFURCATION IN SYNCHRONIZATION OF PERIODIC AND QUASI-PERIODIC OSCILLATIONS THROUGH THE FREQUENCY LOCKING

First, we briefly review the route to synchronization in deterministic self-sustained oscillators. As is well known, a saddle-node bifurcation of limit cycles is the underlying mechanism of frequency locking in the case of a quasi-harmonic oscillator (e.g., a van der Pol oscillator) under external harmonic force in the case of a small external amplitude,¹

$$\ddot{x} - (\lambda - x^2)\dot{x} + x = A_{ex} \sin \omega_{ex} t. \quad (1)$$

Here x is a dynamic variable, λ is a control parameter, A_{ex} and ω_{ex} are the amplitude and the frequency of the external harmonic force, respectively. When the oscillations are not synchronized, an ergodic two-dimensional torus exists in the phase space of (1) (Fig. 1(a)). Inside the synchronization region of the parametric plane, the phase space has the structure shown in Fig. 1(b). There are two limit cycles (stable and unstable) on the surface of the former two-dimensional torus. The transition from synchronization to desynchronization goes through a tangential bifurcation of these limit cycles.

There is a useful approach to treat the bifurcational analysis in this case, namely, via phase reduction. Here, the phase difference between the oscillations of the quasi-

^{a)}Electronic mail: s.v.astakhov@gmail.com.

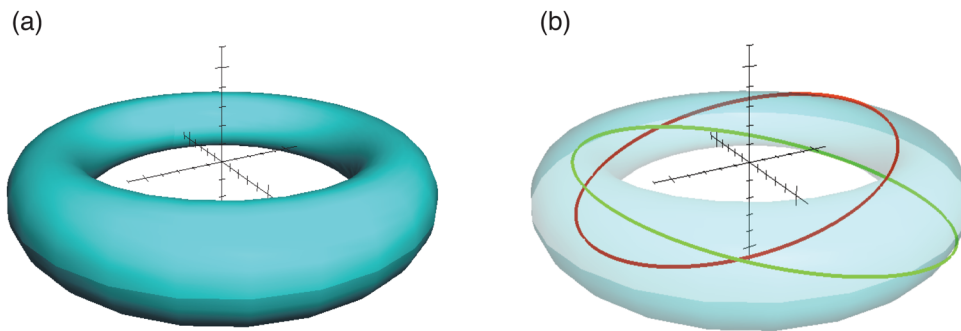


FIG. 1. (Color online) The qualitative phase space structure of a quasi-harmonic oscillator under external harmonic forcing (1): (a) outside synchronization region—ergodic two-dimensional torus; (b) inside synchronization region—stable (light, green online) and unstable (dark, red online) limit cycles on the surface of the former two-dimensional torus.

harmonic self-sustained oscillator and the external force is considered,

$$\dot{\varphi} = -\Delta + \frac{\beta}{\rho} \sin \varphi. \quad (2)$$

Here, φ is the phase difference between the self-sustained oscillations and the external harmonic force, $\Delta = \frac{\omega_{ex}^2 - 1}{2\omega_{ex}}$, ρ is the amplitude of oscillations in Eq. (1), $\beta = \frac{A_{ex}}{2\omega_{ex}}$. Hence, limit cycles are represented by fixed points and a two-dimensional torus by a closed invariant curve in the 2π -periodic phase space of the reduced system. Therefore, the tangential bifurcation of the limit cycles is represented by a saddle-node bifurcation of the fixed points (Fig. 2).

A similar approach can be used to treat a bifurcational analysis of the synchronization mechanisms in the case of quasi-periodic self-sustained oscillations under an external harmonic force,¹⁴

$$\begin{aligned} \ddot{x}_1 + \omega_1^2 x_1 &= (\varepsilon - x_1^2) \dot{x}_1 + \gamma(\dot{x}_2 - \dot{x}_1) + C_0 \cos(\omega_{ex} t), \\ \ddot{x}_2 + \omega_2^2 x_2 &= (\varepsilon - x_2^2) \dot{x}_2 + \gamma(\dot{x}_1 - \dot{x}_2). \end{aligned} \quad (3)$$

Here, $x_{1,2}$ are dynamical variables, ω , ε , γ are control parameters, C_0 and ω_{ex} are the amplitude and frequency of the external force. Applying the phase reduction approach one obtains

$$\begin{aligned} \dot{\varphi}_1 &= \Delta_1 + g \sin(\varphi_2 - \varphi_1) - \frac{C}{\omega_1 - \Delta_1} \cos \varphi_1, \\ \dot{\varphi}_2 &= \Delta_2 + \delta - g \sin(\varphi_2 - \varphi_1), \end{aligned} \quad (4)$$

where $\varphi_{1,2}$ are the phase differences between the oscillations of partial oscillators and external force, $g = \gamma/2$, $\Delta_1 = (\omega_1^2 - \omega_2^2)/(2\omega_{ex}) \simeq \omega_1 - \omega_{ex}$, $\delta = \omega_2 - \omega_1$.

In this case, the phase space of the reduced system becomes two-dimensional and besides the saddle-node bifurcations of equilibrium points there is also a tangential bifurcation of the closed invariant curves (Fig. 3). As the fixed points of Eq. (4) represent the limit cycles in the non-

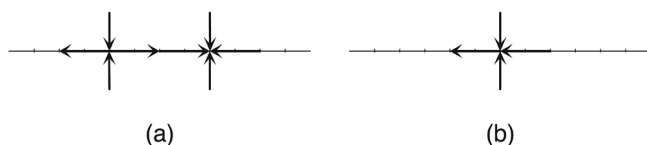


FIG. 2. The phase space structure of the reduced system (2): (a) inside the synchronization region—two fixed points (a saddle and a stable node); (b) outside the synchronization region (no fixed points).

reduced system (3) and closed invariant curves represent two-dimensional ergodic tori, the following sequence of bifurcations takes place. When all three frequencies are locked (two natural frequencies of the self-sustained oscillations and one frequency of the external force), the phase space consists of four limit cycles. Two of them are saddles, one is stable and the other is a repeller. Then, one saddle limit cycle approaches a stable one and another saddle limit cycle approaches the repeller. When a simultaneous tangential bifurcation of pairs of limit cycles takes place, two two-dimensional ergodic tori appear in the phase space. One of them is stable and corresponds to the two-frequency oscillations in the system (two frequencies are locked and one is unlocked) and the other is a saddle. Further variation of the control parameter leads the saddle two-dimensional torus to approach a stable one and their tangential bifurcation. After the bifurcation, only a three-dimensional ergodic torus exists in the phase space (which corresponds to three-frequency oscillations when no frequency is locked).

In the Fourier spectrum of oscillations in such a system, the transition from a three-dimensional torus to a pair of two-dimensional tori corresponds to the locking of one frequency. Here, we have two possible situations: (i) the external force has entrained one of the natural frequencies and

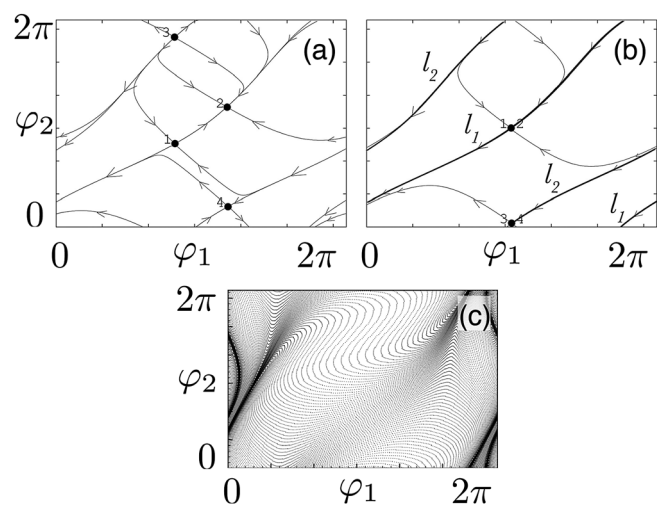


FIG. 3. The phase space structure of the reduced system (4) in the case of two-frequency quasi-periodic self-sustained oscillations under a harmonic force: (a) all frequencies are locked, four fixed points exist on the phase plane; (b) after saddle-node bifurcations of fixed points, only one frequency is locked, two invariant closed curves exist: stable (l_1) and unstable (l_2); (c) after tangential bifurcation of the invariant closed curves, no frequency locking.

(ii) both natural frequencies have locked each other on some mean frequency not equal to the external force frequency. Another transition from two tori to four limit cycles corresponds to the locking of one of the two frequencies by the other one. Hence, one can associate the frequency locking with a tangential bifurcation of some limit sets (whether it would be cycles or tori depend on the number of peaks in the Fourier spectrum).

Keeping this association in mind, we can explain the bifurcation scenario of synchronization in a system which possesses self-sustained oscillations even with a larger number of N independent frequencies, e.g., in an ensemble of quasi-harmonic self-sustained oscillators. For example, one can apply the phase reduction approach to a chain of van der Pol oscillators with open boundaries ($x_0 \equiv x_1, x_6 \equiv x_5$),

$$\ddot{x}_i + \omega_i^2 x_i = \varepsilon(1 - x_i^2)\dot{x}_i + \gamma((\dot{x}_i - \dot{x}_{i-1}) + (\dot{x}_i - \dot{x}_{i+1})), \quad i = 1, \dots, 5 \quad (5)$$

to obtain its phase description,

$$\dot{\varphi}_i = \Delta_i + \frac{\gamma}{2}(\sin(\varphi_i - \varphi_{i-1}) + \sin(\varphi_i - \varphi_{i+1})), \quad i = 1, \dots, 5, \quad (6)$$

where φ_i describes the phase dynamics of the i -th oscillator, Δ_i corresponds to the difference between the natural frequency of the i -th oscillator and some normalized value (e.g., 1), and γ is a coupling coefficient. As the time derivative of the phase φ_i gives the frequency ω_i , one can obtain the bifurcation diagram shown in Fig. 4.¹⁵ Here, each frequency locking can be associated with a tangential bifurcation in the phase space of Eq. (5).

III. SYNCHRONIZATION OF NOISE-INDUCED COHERENT OSCILLATIONS IN AN EXCITABLE MODEL SYSTEM

Let us consider FitzHugh-Nagumo oscillator¹⁶ under the influence of white Gaussian noise,

$$\begin{cases} \varepsilon \frac{dx}{dt} = x - \frac{x^3}{3} - y, \\ \frac{dy}{dt} = x + a + D\xi(t). \end{cases} \quad (7)$$

We choose the following values of control parameters: $\varepsilon = 0.01$ and $a = 1.05$. Then system (7) is in an excitable state. It has been shown¹⁷ that there is a value of noise intensity D for which system (7) generates the mostly coherent oscillations (i.e., the ratio of the height of the main peak in the power spectrum to its width is maximal). This phenomenon is called “Coherence Resonance” (CR). In the CR regime, the oscillations of Eq. (7) are very similar to the oscillations of a noisy quasi-harmonic oscillator (e.g., the van der Pol oscillator under the influence of external Gaussian noise). However, there is an important qualitative difference in the phase space structure of these systems. The FitzHugh-Nagumo oscillator in the excitable state does not have a stable limit cycle (only a stable focus), while self-sustained quasi-harmonic oscillators are characterized by a stable limit cycle.

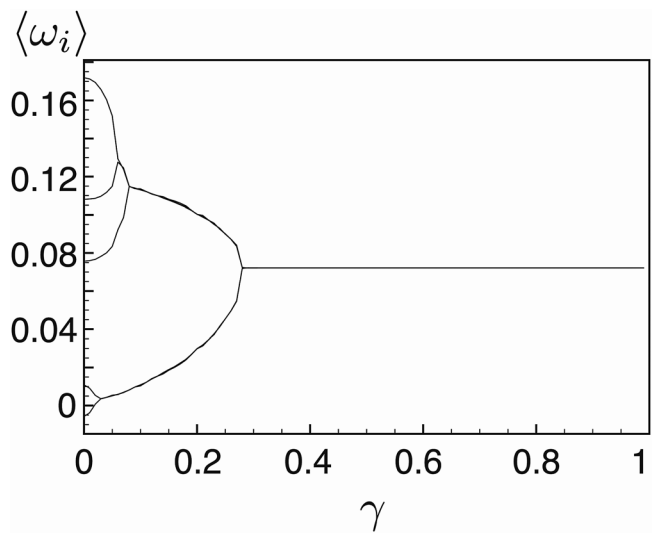


FIG. 4. Mean frequencies versus coupling coefficient in system (6). The value of $\langle \omega_i \rangle$ is given by the right-hand side of Eq. (6) averaged over the integration time interval.

Nevertheless, the oscillations in Eq. (7) in the coherence resonance regime can be synchronized¹⁸ (both external and mutual synchronization) through frequency locking. As the coherence resonance regime captures the main features of a limit cycle (the trajectories starting from the initial conditions picked in the neighborhood of a bounded region tend to this region, and oscillations characterized by a certain averaged frequency can be synchronized), we call it *noise-induced limit cycle*. Therefore, we could extrapolate our association of frequency locking with a tangential bifurcation to the case of synchronization of noise-induced oscillations through a frequency entrainment mechanism. However, if this association is correct, synchronization of noise-induced oscillations with more than one main frequency should obey the same scenario as in case of deterministic quasi-periodic oscillations reviewed in Sec. II. This will be clarified in the following.

Let us analyze a system of two interacting FitzHugh-Nagumo type oscillators in an excitable regime under external white Gaussian noise and an external harmonic force applied to one of the oscillators,

$$\begin{cases} \dot{x}_1 = a_1(b - cx_1 - y_1) + C(x_2 - x_1) + \sqrt{2D}\xi(t) + A_{ex} \cos(\omega_{ex}t), \\ \dot{y}_1 = d(x_1 - F(y_1)), \\ \dot{x}_2 = a_2(b - cx_2 - y_2) + C(x_1 - x_2) + \sqrt{2D}\xi(t), \\ \dot{y}_2 = d(x_2 - F(y_2)), \\ F(y) = \alpha y^3 + \gamma y, \end{cases} \quad (8)$$

where $a_{1,2}, b, c, d, \alpha, \gamma$ are control parameters, C is the coupling coefficient, $\xi(t)$ is a source of white Gaussian noise with intensity D , A_{ex} , and ω_{ex} are the amplitude and the frequency of the external force, respectively. The coupling introduced in system (8) is different from the one introduced in Ref. 18 in order to meet an electronic model presented in Fig. 7. We choose the following values of the parameters: $a_1 = 10^{-4}$, $a_2 = 1.25 \cdot 10^{-4}$, $b = 4.395$, $c = 100$, $d = 10^4$, $\alpha = 2.22 \cdot 10^{-5}$, $\gamma = -1.61 \cdot 10^{-3}$, $D = 10^{-9}$, and vary the

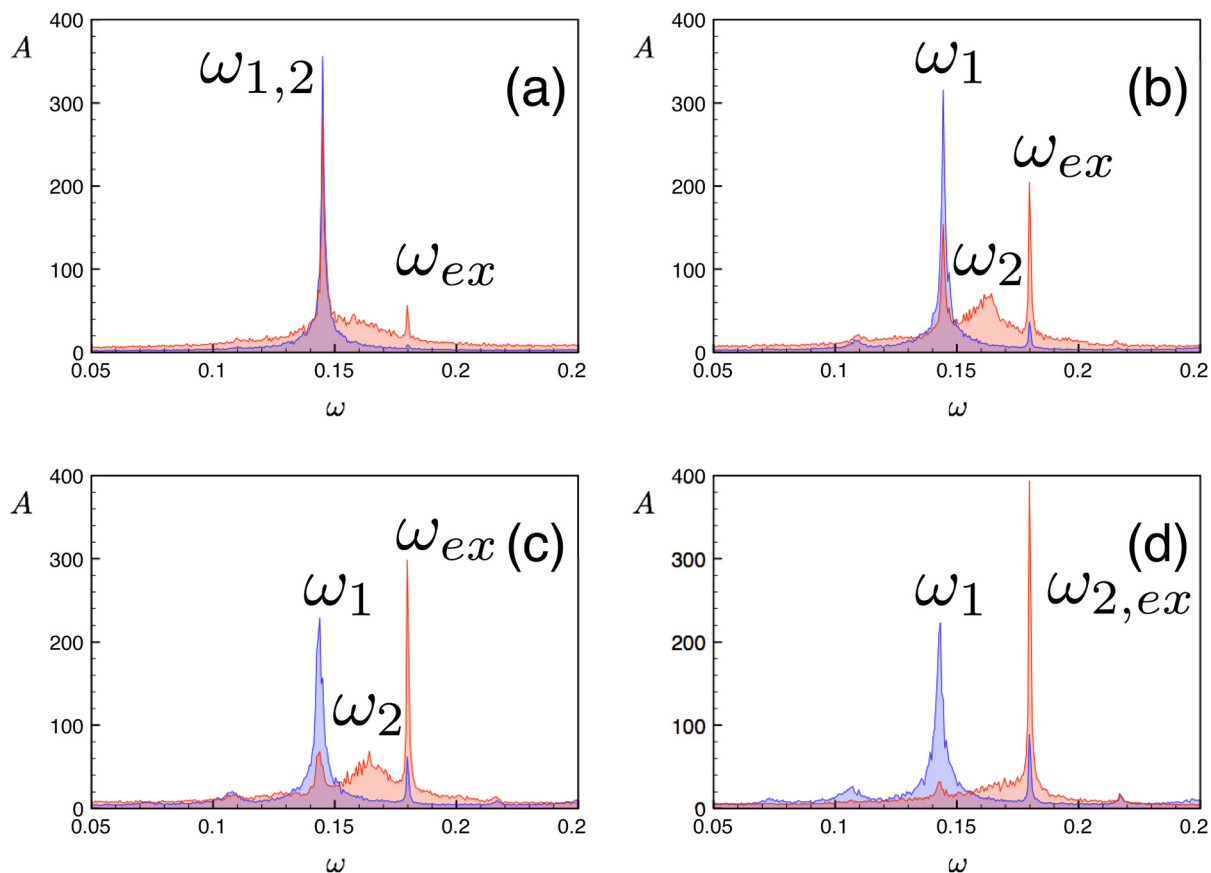


FIG. 5. (Color online) The Fourier spectrum evolution for system (8) calculated for variables x_1 (dark grey, blue in color) and x_2 (light grey, red in color). Here, $\omega_{1,2}$ are mean frequencies of the first and second subsystems, respectively; ω_{ex} is frequency of the external forcing; A_{ex} is amplitude of the external forcing: (a) $A_{ex} = 10^{-5}$ (lower region T^2 in Fig. 6); (b) $A_{ex} = 4 \cdot 10^{-5}$ (region T^3 in Fig. 6); (c) $A_{ex} = 6 \cdot 10^{-5}$ (region T^3 in Fig. 6); (d) $A_{ex} = 8 \cdot 10^{-5}$ (upper region T^2 in Fig. 6).

external harmonic force amplitude A_{ex} and frequency ω_{ex} . The chosen noise intensity value corresponds to the CR regime in each interacting oscillator in Eq. (8).

The Fourier spectra of the oscillations in Eq. (8) are presented in Fig. 5. As one can see from Figure 5, the same frequency locking mechanism indeed appears in the case of three main frequencies. Increasing A_{ex} , one unlocks the frequency of the first oscillator entrained by the second one and then the external harmonic force locks the frequency of the first oscillator. Our parametrical study of Eq. (8) yields the bifurcation diagram shown in Fig. 6. As is easy to see, this bifurcation diagram is topologically equivalent to the one obtained for the deterministic van der Pol oscillators in the phase approach.¹⁴ Using the analogy between self-sustained periodic oscillators and noise-excitable systems in CR and associating frequency entrainment with a tangential bifurcation of invariant limit sets, the transition from C to T^3 in Fig. 6 can be explained as follows. In region C , the phase space of Eq. (8) contains four noise-induced limit cycles: two are saddles, one is stable and the other is a repeller. The transition from region C to region T^2 corresponds to simultaneous tangential bifurcations between saddle and stable and between saddle and repeller noise-induced limit cycles. As a result, two noise-induced two-dimensional tori appear: a stable torus and a saddle torus. The oscillations on the stable noise-induced two-dimensional torus are characterized by two frequencies and two main peaks in the Fourier spectrum

(Fig. 5(a)). Approaching the border between T^2 and T^3 makes the noise-induced tori approach each other and a transition from T^2 to T^3 corresponds to their tangential bifurcation, resulting into a noise-induced three-dimensional torus

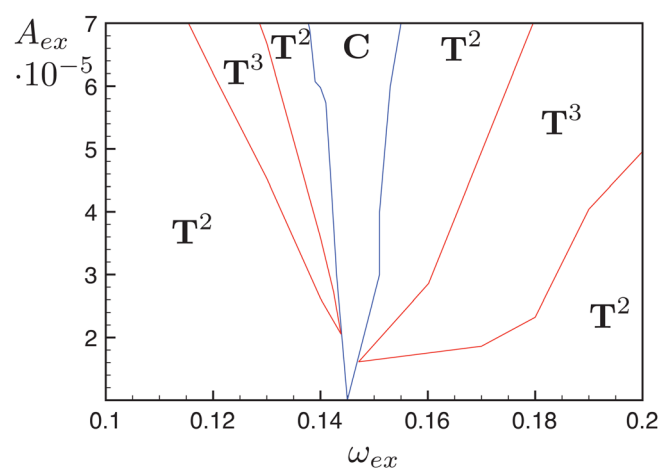


FIG. 6. (Color online) The bifurcation diagram of system (8). Region C : one main frequency in the spectrum, both frequencies of noise-induced oscillations entrained by an external harmonic force. Regions T^2 : two main frequencies in the spectrum, either one oscillator is synchronized by the external force at a frequency which differs from that of the other oscillator, or both oscillators are mutually synchronized at a frequency different from external forcing frequency. Regions T^3 : three main frequencies in the spectrum, no synchronization in the system.

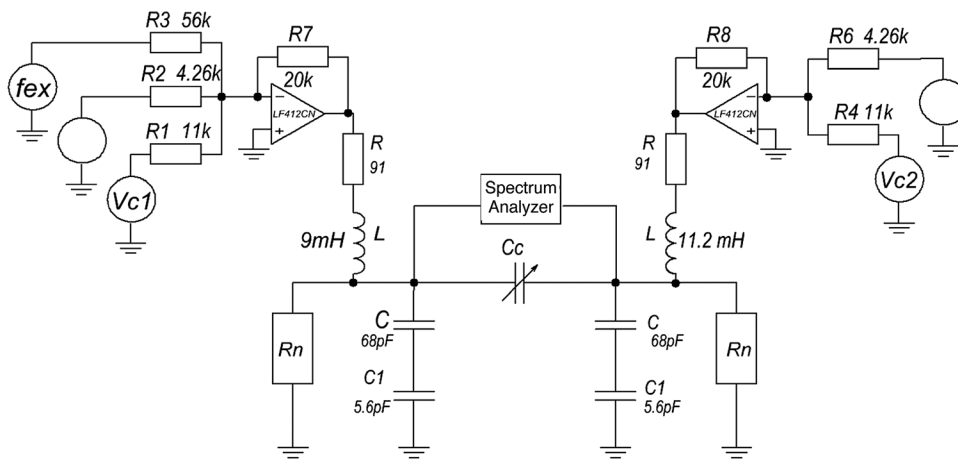


FIG. 7. Electronic setup modeling the dynamics of system (8).

in the phase space and three main frequencies in the spectrum (Fig. 5(b)).

IV. EXPERIMENT

We confirmed our results experimentally, using the electronic scheme presented in Fig. 7. The experimental setup is represented by two coupled subsystems. Each subsystem is based on the original scheme proposed by FitzHugh and Nagumo.¹⁶ However, to model the N-characteristic of the nonlinear element, we used an operational amplifier. Hence, the partial subsystem consists of the capacitors C , $C1$, the inductor L , the resistor R , the nonlinear element with N-characteristic and the adder based on an operational amplifier LF412. Voltage Vc and noise are applied to the adder. The nonlinear element is also based on an operational amplifier LF412.

As is clearly seen from Fig. 7, the scheme is symmetric, as it is represented by two almost identical coupled subsystems. The only difference between the subsystems is the value of inductance L : $L = 9$ mH for the first subsystem and $L = 11$ mH for the second one. An external harmonic signal is applied to the adder of the first subsystem. The coupling between subsystems is realized through a capacitor Cc , whose capacity value can be varied. The signals from each subsystem are directed to different input channels of the spectrum analyzer.

We fixed the following values of voltages $Vc1 = 2.39$ V, $Vc2 = 2.84$ V and the coupling capacity: $Cc = 42.37$ pF. Then we changed the amplitude and frequency of the external harmonic signal to observe frequency lockings with the help of a spectrum analyzer. The experimentally obtained bifurcation diagram is shown in Fig. 8. It is clearly seen that our electronic experiment proves the results of our numerical studies.

V. ENSEMBLE OF EXCITABLE MODEL SYSTEMS

In Sec. II, we also mentioned a sequence of frequency lockings in an ensemble of non-identical van der Pol oscillators. If our assumption that noise-induced limit cycles and tori demonstrate bifurcations similar to the deterministic ones is correct, then a similar sequence of frequency lockings has to be expected in an ensemble of five non-identical (in a_i) excitable systems under external noise in the vicinity

of coherence resonance. To clarify this, we consider the following system:

$$\begin{cases} \dot{x}_i = a_i(b - cx_i - y_i) + C(x_i - \sum_{j=1}^5 x_j) + \sqrt{2D}\xi(t), \\ \dot{y}_i = d(x_i - F(y_i)), \\ F(y) = \alpha y^3 + \gamma y. \end{cases} \quad (9)$$

We fix the following values of control parameters: $a_1 = 10^{-4}$, $a_2 = 1.1 \cdot 10^{-4}$, $a_3 = 1.25 \cdot 10^{-4}$, $a_4 = 1.35 \cdot 10^{-4}$, $a_5 = 1.5 \cdot 10^{-4}$, $b = 4.395$, $c = 100$, $d = 10^4$, $\alpha = 2.22 \cdot 10^{-5}$, $\gamma = -1.61 \cdot 10^{-3}$, $D = 10^{-9}$. Here, the noise level D corresponds to the CR regime in each subsystem. Then we increase the value of the coupling coefficient C . The tree-like diagram similar to the one in Fig. 4 is shown in Fig. 9. This similarity allows us to hypothesize that there is indeed a sequence of tangential bifurcations of noise-induced tori which underlies a transition from one main frequency to 5 frequencies in the spectrum.

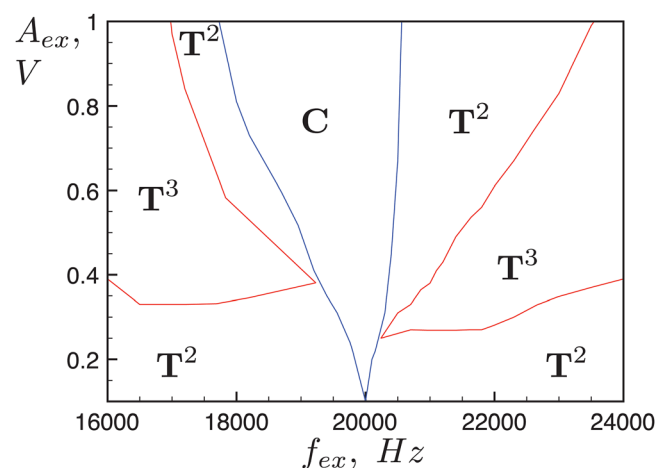


FIG. 8. (Color online) The bifurcation diagram obtained from the electronic experiment. Region C: one main frequency in the spectrum, both frequencies of noise-induced oscillations entrained by an external harmonic force. Regions T^2 : two main frequencies in the spectrum—either one oscillator is synchronized by the external force at a frequency which differs from the frequency of the other oscillator or both oscillators are mutually synchronized on the frequency different from external force frequency. Regions T^3 : three main frequencies in the spectrum, no synchronization in the system.

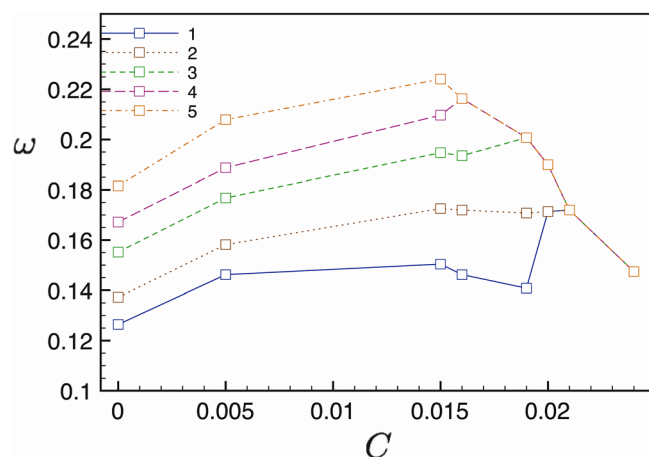


FIG. 9. (Color online) Frequencies versus coupling coefficient in system (9).

VI. CONCLUSION

The results presented in this paper show that noise-induced oscillations of excitable systems which have more than one main peak in the Fourier spectrum demonstrate a synchronization route through frequency entrainments which is similar to the case of deterministic quasi-periodic oscillations. As in the case of quasi-periodic oscillations, where a sequence of tangential bifurcations of cycles and tori underlies the synchronization route, we hypothesize that stable and unstable noise-induced limit-cycles and invariant tori do exist in the phase space and perform a similar sequence of tangential bifurcations in excitable systems.

We show such an analogy also for synchronization in ensembles of non-identical excitable elements under the influence of noise. This is of special practical interest. The synchronization mechanism allows one to unlock any of the entrained frequencies by applying an external harmonic force at a frequency close to the natural frequency of a certain oscillator. Synchronization phenomenon plays a big role in neuroscience, sometimes even a destructive role. In case of Parkinson's disease, the temporal evolution of the peripheral tremor rhythms corresponds to abnormal activity between cortical motor areas.⁶ Epileptic seizures also can result from synchronized neural activity.¹⁹ As the FitzHugh-Nagumo oscillator represents one of the basic neural models, one could be able to desynchronize a single neuron in an en-

semble by appropriately applying an external harmonic force. It may be interesting to carry out such an experiment in neuroscience. The combination of neuroscience and nonlinear dynamics in these experiments in future will represent the full maturity of a field that owes its success in large part to the valuable contributions of Frank Moss.^{4,5}

ACKNOWLEDGMENTS

S.A. and V.A. are grateful for the financial support of the Alexander von Humboldt Foundation and Russian Ministry of Education and Sciences (Grant No. 2.2.2.2/11514) and J.K. for the support by the federal ministry of education and research Germany (BCCN2, Grant No. 01GQ1001A). The authors dedicate this paper to the genuine memory of Frank Moss.

- ¹A. Pikovsky, M. Rosenblum, and J. Kurths, *Synchronization: A Universal Concept in Nonlinear Science* (Cambridge University Press, Cambridge, 2003).
- ²D. Mertens and R. Weaver, *Phys. Rev. E* **83**, 046221 (2011).
- ³A. Feoktistov, S. Astakhov, and V. Anishchenko, in *17th International Workshop on Nonlinear Dynamics of Electronic Systems* (Rapperswil, Switzerland, 2009), pp. 114–117.
- ⁴A. Neiman, X. Pei, D. Russell, W. Wojtenek, L. Wilkens, F. Moss, H. A. Braun, M. T. Huber, and K. Voigt, *Phys. Rev. Lett.* **82**, 660 (1999).
- ⁵A. Neiman, L. Schimansky-Geier, A. Cornell-Bell, and F. Moss, *Phys. Rev. Lett.* **83**, 4896 (1999).
- ⁶P. Tass, M. G. Rosenblum, J. Weule, J. Kurths, A. Pikovsky, J. Volkmann, A. Schnitzler, and H.-J. Freund, *Phys. Rev. Lett.* **81**, 3291 (1998).
- ⁷M. Wickramasinghe and I. Z. Kiss, *Phys. Rev. E* **83**, 016210 (2011).
- ⁸C. Zhou, J. Kurths, I. Z. Kiss, and J. L. Hudson, *Phys. Rev. Lett.* **89**, 014101 (2002).
- ⁹G. S. Duane and J. J. Tribbia, *Phys. Rev. Lett.* **86**, 4298 (2001).
- ¹⁰D. Maraun and J. Kurths, *Geophys. Res. Lett.* **32**, L15709 (2005).
- ¹¹I. I. Mokhov, D. A. Smirnov, P. I. Nakonechny, S. S. Kozlenko, E. P. Seleznev, and J. Kurths, *Geophys. Res. Lett.* **38**, L00F04 (2011).
- ¹²M. McDonald, O. Suleman, S. Williams, S. Howison, and N. F. Johnson, *Phys. Rev. E* **77**, 046110 (2008).
- ¹³W.-X. Wang, X. Ni, Y.-C. Lai, and C. Grebogi, *Phys. Rev. E* **83**, 011917 (2011).
- ¹⁴V. Anishchenko, S. Astakhov, and T. Vadivasova, *Europhys. Lett.* **86**, 30003 (2009).
- ¹⁵M. Giver, Z. Jabeen, and B. Chakraborty, *Phys. Rev. E* **83**, 046206 (2011).
- ¹⁶R. FitzHugh, *Bull. Math. Biol.* **17**, 257 (1955).
- ¹⁷A. Pikovsky and J. Kurths, *Phys. Rev. Lett.* **78**, 775 (1997).
- ¹⁸C. Zhou, J. Kurths, and B. Hu, *Phys. Rev. E* **67**, 030101 (2003).
- ¹⁹D. Takeshita, Y. D. Sato, and S. Bahar, *Phys. Rev. E* **75**, 051925 (2007).